Acta Crystallographica Section D
Biological Crystallography
ISSN 0907-4449

MAD on threonine synthase: the phasing power of oxidized selenomethionine

Karine Thomazeau,[a] Gilles Curien,[b] Andrew Thompson,[c] Renaud Dumas[b] and Valérie Biou[a]*

[a]Institut de Biologie Structurale Jean-Pierre Ebel, UMR 5075 CNRS–CEA–Université Joseph Fourier, 41 Rue Jules Horowitz, F-38027 Grenoble CEDEX 1, France, [b]UMR 1932 CNRS–INRA–Aventis CropScience, 14–20 Rue Pierre Baizet, F-69263 Lyon CEDEX 9, France, and [c]EMBL Grenoble Outstation, 6 Rue Jules Horowitz, BP181, F-38042 Grenoble CEDEX 9, France

Correspondence e-mail: biou@ibs.fr

Received 1 March 2001
Accepted 25 May 2001

PDB Reference: threonine synthase, 1e5x.

The use of selenomethionine and anomalous dispersion has become the most widely used way of solving the phase problem for *de novo* protein structure determination. In this paper, MAD data collected from oxidized and reduced selenomethionine-containing protein are described, and it is shown that oxidized selenomethionine has a very strong phasing power and can be efficiently used if the oxidation is uniform. The comparison was performed on threonine synthase crystals. For example, the phasing power of the oxidized data is doubled for the dispersive signal and is 20% stronger for the anomalous signal at the peak wavelength. The strength of the anomalous signal can be used to improve the signal when a protein contains few methionines or for single anomalous dispersion. The oxidation of some selenomethionines shows in the electron-density map through the presence of water molecules within hydrogen-bonding distance of the putative O atom.

1. Introduction

The use of the anomalous diffraction of selenomethionine has become the most widely used way of solving the phase problem in protein crystallography. A mixture of oxidized and reduced selenomethionine residues in the same crystal has been shown to be deleterious for the phasing power of a MAD experiment. Most often, users try to avoid oxidizing selenomethionine by using reducing agents such as DTT or β-mercaptoethanol (Smith & Thompson, 1998). However, deliberately oxidized selenomethionine has been used to improve the phasing power and solve the structure of TolC protein (Sharff *et al.*, 2000). In order to determine if oxidized selenomethionine could be used routinely, we have compared the phasing powers of oxidized and reduced selenomethionine. This study formed part of the structure determination of threonine synthase (Thomazeau *et al.*, 2001).

Threonine synthase (TS) is a pyridoxal 5′-phosphate (PLP) dependent enzyme which catalyses the last step of threonine formation. It converts *O*-phospho-L-homoserine (OPH) to threonine and inorganic phosphate. In plants, OPH is the branch-point intermediate between threonine and methionine pathways. The plant TS is a homodimeric enzyme of 116 kDa strongly activated by *S*-adenosylmethionine (SAM), the final product of methionine synthesis. This activation does not exist with the bacterial enzyme, where the branch point is located upstream. To understand how such an activation is possible, structural studies were undertaken by attempting to crystallize a plant TS enzyme with or without its effector SAM.

In this paper, we report the production and crystallization of selenomethionine-substituted (14 Met residues in 58 kDa) apoTS from *Arabidopsis thaliana* and compare the phasing power of oxidized and reduced selenomethionine in MAD experiments.

2. Experimental conditions and results

2.1. Expression and purification

Native threonine synthase from *A. thaliana* was expressed using the pKKTSmat plasmid and purified as described previously (Curien *et al.*, 1998). Pure enzyme (in 20 m*M* HEPES–KOH pH 7.5) was concentrated on Microsep 30K (Pall Filtron) to a concentration of 20 mg ml^{-1} and stored at 193 K. The selenomethionine-substituted enzyme was overproduced in a different way. The nucleotide sequence corresponding to the mature enzyme was constructed by PCR using the pKKTSmat plasmid with a proofreading PWO polymerase. The oligonucleotide corresponding to the coding sequence was designed to have an *Nco*I restriction site with insertion of ATG instead of the codon corresponding to the first amino acid of the mature *A. thaliana* sequence (Thr40). The oligonucleotide corresponding to the complementary sequence was constructed in order to insert a *Hin*dIII restriction site after the TGA stop codon. The PCR product was *Nco*I/*Hin*dIII digested and cloned into a

pET23d plasmid to give pET23TS. Transformed *E. coli* strain B834-DE3 (methionine auxotroph) was used for recombinant protein overproduction. Cells were grown at 301 K in 1 l LB medium supplemented with carbenicillin (100 µg µl^{-1}). The cells were harvested by centrifugation when bacterial growth was equivalent to an A_{600} of 0.15. The pellet was washed and resuspended in M9 medium. The cells were grown at 301 K in 1 l of M9 medium supplemented with amino acids (40 mg each; 19 amino acids except methionine), selenomethionine (14 mg), glucose (40 g), vitamins (thiamine, 1 mg; pyridoxine, 1 mg), salts (2 m*M* $MgSO_4$; 0.1 m*M* $CaCl_2$) and carbenicillin (100 mg). After 30 min, induction was initiated with isopropyl-β-thiogalactoside (0.4 m*M*) and the cells were grown for a further 20 h at 301 K.

The preparation of the selenomethionine enzyme was identical to those described for TS enzyme except that purification was carried out in one step on a DEAE EMD 650 column (2.6 × 30 cm; Sigma) using degassed buffers (with argon) containing 5 m*M* DTT. Purified selenated enzyme (in 20 m*M* HEPES–KOH pH 7.5, 5 m*M* DTT) was concentrated on Microsep 30K to a concentration of 20 mg ml^{-1} and stored at 193 K until use. The full substitution of the methionine residues with selenomethionine was confirmed by electrospray mass spectrometry from the protein solution. The measured mass of 53 986 Da corresponded to the fully selenated protein plus one PLP molecule. An additional 96 Da was interpreted as corresponding to partial selenomethionine oxidation (six O atoms).

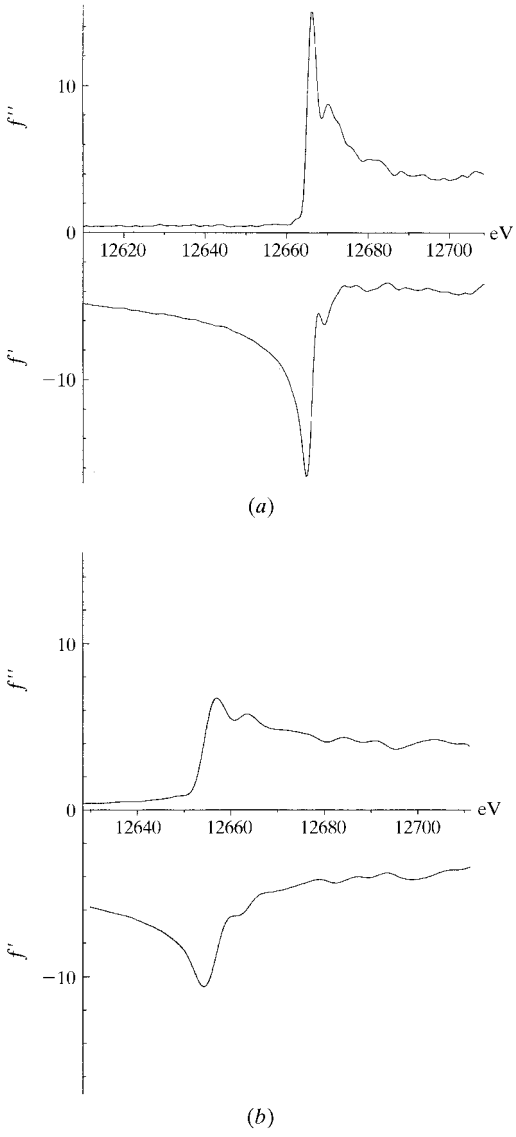

Figure 1
Scattering factors (f' and f'') from TS crystals. (*a*) Oxidized crystal; (*b*) reduced crystal. The energy indicated corresponds to the beamline calibration.

2.2. Crystallization and crystal characterization

All crystals were grown using the hanging-drop vapour-diffusion technique at 293 K. Crystals from threonine synthase were obtained from the PEG/LiCl kit conditions (Hampton Research). Optimized conditions were obtained by reducing the volume of the hanging drop from 6 to 3 µl. To produce these crystals, 1.5 µl protein solution (5.4 µg TS in 20 m*M* HEPES pH 7.5, 5 m*M* DTT) was mixed with 1.5 µl reservoir solution (13% PEG 6000, 0.1 *M* MES pH 6.5, 1 *M* LiCl, 5 m*M* DTT). All reservoir solutions were bubbled through with argon before adding 5 m*M* DTT. Crystals appear within 10 d and grow to approximately 100 × 80 × 50 µm.

Flash-cooling conditions were established by adding 10% glycerol to a reservoir-like solution (15% PEG 6000, 0.1 *M* MES pH 6.5, 1 *M* LiCl). A first complete native data set was collected to 2.5 Å resolution from one crystal cryocooled to 100 K. The crystals belong to space group *P*1, with unit-cell parameters a = 57.8, b = 62.2, c = 76.5 Å, α = 109.4, β = 97.6, γ = 112.9°. Assuming one dimer per asymmetric unit, the Matthews coefficient V_M was calculated to be 2.00 Å^3 Da^{-1}, corresponding to a solvent content of 38%. The selenomethionine-substituted enzyme crystallized under similar conditions with an optimal pH of 6.2.

2.3. Data collection using oxidized and reduced selenomethionine

2.3.1. Fluorescence spectra and anomalous signal. Two MAD data sets were collected from crystals of the selenomethionine protein. The first fluorescence scan measured from a crystal on beamline BM14 at the ESRF showed a strong oxidation of the selenomethionine and the MAD data collected on oxidized crystals permitted structure solution. Two weeks later, we had the opportunity to collect data on beamline BM30 and chose to soak a crystal with 5 m*M* DTT for 30 min because we thought non-homogeneous oxidization could cause a problem in phase determination. The fluorescence spectrum was typical of reduced selenomethionine. Again, the MAD data permitted structure solution. The fluorescence spectra have been converted into electron units in order to visualize the f' and f'' scattering factors using the program *CHOOCH* (Evans & Pettifer, 2001). Fig. 1 shows the absorption spectra of oxidized (Fig. 1*a*) and reduced (Fig. 1*b*) crystals. The maximum value for f'' is 15 electron units and the f' minimum is −16.5 electron units for the oxidized crystal. f''_{max} is 6.7 and f'_{min} is −10.7 electrons for the reduced crystal. The full-width at half-maximum of the white line is typical of a fully reduced or fully oxidized selenomethionine, compared with the spectra published on TolC (Sharff *et al.*, 2000) and observed on other reduced proteins. We can therefore suppose that the protein was fully oxidized in the untreated crystals and became fully reduced upon soaking with 5 m*M* DTT for 30 min. The oxidation of the crystals occurred despite the addition of DTT and despite the use of argon bubbling through all reservoir solutions.

The calculation of the theoretical dispersive and anomalous signals according to the relations dispersive ratio = $q \times (f'_{l1} - f'_{l2})$ and anomalous ratio = $q \times 2f''$ [where $q = (1/Z_{eff})(N_a/2N_p)^{1/2}$, N_a is the number of anomalous scatterers, N_p is the number of protein atoms, Z_{eff} is the effective normal scattering, f' is the dispersive scattering factor and f'' is the anomalous scattering factor; Hendrickson *et al.*, 1985] shows that the anomalous ratio is 19 and 8% for the oxidized and reduced data, respectively, and that the dispersive ratio is 8.4 and 4.3% for the oxidized and reduced data, respectively. Therefore, using oxidized selenomethionine would permit phasing of twice as many

Table 1
Data-collection statistics for both MAD data sets.

Oxidized, data measured from untreated crystal; reduced, data measured from crystal soaked with DTT. Values in parentheses are for the outer resolution shell.

	Oxidized MAD data set			Reduced MAD data set		
Unit-cell parameters (Å,°)	57.8, 62.1, 76.6; 109.5, 97.6, 112.7			57.8, 62.2, 76.8; 109.5, 97.5, 112.8		
Wavelength (Å)	0.9788 (peak)	0.9789 (edge)	0.886 (remote)	0.9795 (peak)	0.9797 (edge)	0.9729 (remote)
Resolution (Å)	20–2.20	20–2.20	20–2.25	20–2.53	20–2.53	20–2.50
No. of reflections	172124 (24511)	170855 (23454)	124846 (17896)	105840 (6600)	106729 (6626)	108563 (9293)
No. of unique reflections	43625 (6233)	43254 (5954)	43719 (6265)	28359 (3129)	28358 (3223)	29154 (3953)
Completeness (%)	97 (94.8)	96.6 (93.5)	97.2 (95.3)	95.7 (85.6)	96.3 (88.2)	95.8 (88.8)
Multiplicity	3.9 (3.9)	4.0 (3.9)	2.9 (2.9)	3.7 (2.1)	3.7 (2.1)	3.7 (2.4)
R_{sym}†	0.042 (0.256)	0.036 (0.184)	0.033 (0.183)	0.053 (0.151)	0.050 (0.100)	0.046 (0.113)
R_{ano}‡	0.074 (0.192)	0.050 (0.129)	0.042 (0.139)	0.073 (0.133)	0.044 (0.109)	0.047 (0.112)
Anomalous completeness	96.6 (94.5)	96.4 (93.3)	95.7 (93.8)	90.5 (49.7)	93.5 (68.1)	92.6 (71.2)

† $R_{sym} = \sum_j |\bar{I} - I_j| / \sum_j \bar{I}$, where I is the intensity of the jth observation and $\bar{I}$ is the average intensity over all observations. ‡ $R_{ano} = \sum |\overline{I_+} - \overline{I_-}| / \sum (\overline{I_+} + \overline{I_-})$.

Table 2
MAD phasing statistics using *SHARP*.

ISO, isomorphous differences; ANO, anomalous differences. Oxidized, data collected on non-reduced crystals (20–2.25 Å data); Oxidized 2.5 Å, same data set truncated to 2.5 Å resolution for comparison with reduced figures. Reduced, data collected on crystals treated with DTT prior to flash-cooling (20–2.5 Å data). The overall figure of merit for the oxidized data was 0.67 to 2.2 Å resolution and for the 'reduced' data was 0.68 to 2.5 Å resolution.

	Remote		Peak		Edge	
Wavelength	ISO	ANO	ISO	ANO	ISO	ANO
R_{Cullis}†, oxidized		0.74	0.69	0.56	0.40	0.77
R_{Cullis}, oxidized 2.5 Å		0.68	0.44	0.50	0.30	0.58
R_{Cullis}, reduced		0.75	0.50	0.60	0.35	0.67
R_{Kraut}‡, oxidized	0.019	0.042	0.033	0.063	0.024	0.047
R_{Kraut}, oxidized 2.5 Å	0.016	0.033	0.024	0.047	0.019	0.034
R_{Kraut}, reduced	0.017	0.046	0.037	0.052	0.020	0.042
Phasing power§, oxidized		2.1	3.6	2.9	4.5	2.4
Phasing power, oxidized 2.5 Å		2.6	4.8	3.7	5.8	3.0
Phasing power, reduced		2.0	2.4	3.1	4.4	2.1

† $R_{Cullis} = \sum ||F_{PH} \pm F_P| - |F_{PH(calc)}|| / \sum |F_{PH} - F_P|$. ‡ $R_{Kraut} = \sum ||F_{PH} \pm F_P| - |F_{PH(calc)}|| / \sum |F_{PH}|$. § Phasing power = $|F_{H(calc)}| / \sum ||F_{PH} \pm F_P| - |F_{PH(calc)}||$.

atoms than reduced methionine for similar quality data.

A word of caution is necessary to compare the spectra. They have been measured on two different beamlines with different monochromator calibration, which explains the difference in energy as seen in Fig. 1. Therefore, it is meaningless to plot them on the same graph. However, the comparison of the edge heights is meaningful, since the two beamlines have almost equivalent energy resolutions ($\Delta E/E \simeq 2 \times 10^{-4}$, beamline description at http://www.esrf.fr; Ferrer *et al.*, 1998; A. Thompson, unpublished data).

2.4. Diffraction data

Good-quality data were measured at three wavelengths from both oxidation conditions (see Table 1). Owing to the *P*1 space group, redundancy was limited to less than 4 as a compromise in order to collect 360° from each wavelength on the same crystal without causing too much radiation damage.

2.4.1. Oxidized data set. Data were collected on synchrotron beamline BM14 at the ESRF using a MAR CCD detector. The diffraction images were processed using the program *DENZO* (Otwinowski, 1993) and merged with *SCALA* (Evans, 1997). The results are summarized in Table 1. The crystal diffraction limit was 2.2 Å. The remote wavelength was used as a reference in phasing.

2.4.2. Reduced data set. Data were collected on beamline BM30 at the ESRF using a MAR Research imaging-plate detector. In order to reduce scan time, the detector size was set to 180 mm, thus limiting the resolution to 2.5 Å. The images were integrated using the program *MOSFLM* (Leslie, 1990) and scaled with *SCALA*.

2.4.3. Phasing statistics. As stated previously, both MAD data sets allowed structure solution. 26 of 28 Se atoms were located using difference maps starting from one atom positioned at (0, 0, 0). The missing two proved to be located on a disordered loop on each monomer. Preliminary phase calculations were performed with *MLPHARE* (Otwinowski, 1991) and final refinements of heavy-atom parameters and phase calculation were performed with *SHARP* (de La Fortelle *et al.*, 1997). Table 2 shows phasing statistics from *SHARP*. It is interesting to compare both data sets at the same resolution ('oxidized 2.5 Å' and 'reduced' lines). They show that oxidized selenomethionine indeed has a much stronger phasing power than its reduced form. For example, the anomalous phasing powers of the oxidized peak and inflexion wavelengths are 20 and 43% stronger, respectively. The dispersive signal of the oxidized peak wavelength is twice as strong as that of the reduced one, but this includes the influence of a very remote wavelength as a reference in the oxidized data set. The oxidized map at 2.2 Å allowed tracing of the model and the refinement was successful (Thomazeau *et al.*, 2001).

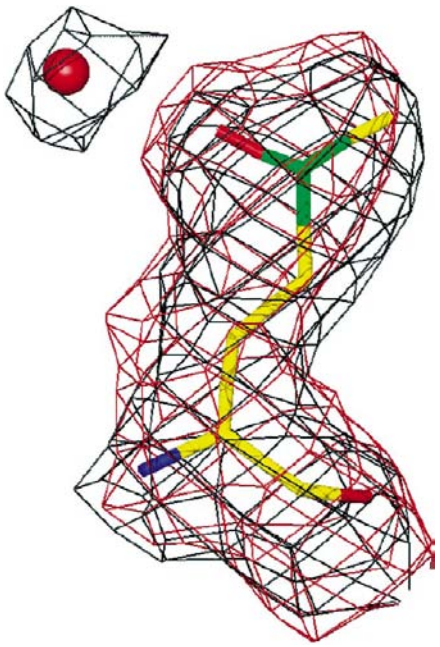

Figure 2
MAD electron-density maps of oxidized and reduced selenomethionine. The maps were contoured at 1 root-mean-square deviation. The oxidized map is in black and the reduced map in red. The model shows threonine synthase oxidized selenomethionine 309 as present in the refined model. The figure was produced using *O* (Jones *et al.*, 1991) and the *Molray* server at Uppsala University (http://xray.bmc.uu.se/molray).

2.4.4. Electron-density maps. The comparison of the raw MAD electron-density maps allows the visualization of oxidized selenomethionine in several cases. One obvious marker is the presence of electron density for a water molecule in the vicinity of the ε position. For example, residue 309 from both monomers shows a water molecule that hydrogen bonds to the additional O atom. This water molecule is present in the oxidized electron-density map and is absent from the reduced map (see Fig. 2). The structure refinement gave a lower R factor and $R_{\rm free}$ upon addition of the O atom to the selenomethionine residue and water molecule. Other residues showed more subtle differences, such as more bulky oxidized electron density. Yet others showed no obvious differences. Three rotamers of the six defined in a recently published rotamer library (Lovell *et al.*, 2000) can be fitted into the electron density of most selenomethionines. Those rotamers correspond to variable positions of the CE atom with respect to the beginning of the side chain. The spherical shape of the density can be interpreted as the co-existence of the three rotamers and is compatible with the presence of an O atom. This situation is less favourable for a water molecule to bind in an ordered way.

Selenomethionine oxide has been shown to be easily reduced by mercaptoethanol or glutathione (Sies *et al.*, 1998). This work shows two points that can be useful for phase determination using selenomethionine anomalous properties. Firstly, it is also easily reduced by DTT, but owing to the instability of DTT this reduction is reversible. Secondly, oxidized selenomethionine is indeed a good phasing tool when it is homogeneous. Our comparison of the phasing powers of both oxidation states shows that it is possible to obtain fully oxidized and fully reduced species. Selenomethionine oxidation can make the difference in difficult cases such as when the protein contains few methionines, as has been shown in other recent work (Sharff *et al.*, 2000), or when single anomalous dispersion (SAD) is necessary because of radiation damage or lack of time. Note that the space group of the crystals ($P1$) makes it unlikely that differences in phasing power might be a consequence of different data-collection strategies (*e.g.* set *versus* inverse-beam orientation). In addition, the intensities of the two bending-magnet beamlines BM14 and BM30 are similar, so it is unlikely that differences would be a consequence of radiation-damage effects. In any event, we would expect the selenomethionine-oxidized form to be more radiation sensitive than the reduced form.

We thank Franck Fieschi for helpful discussions. We thank Vivian Stojanoff for her help in using beamline BM14 and Richard Kahn for his help in using beamline BM30 at the European Synchrotron Radiation Facility (ESRF) in Grenoble. We acknowledge support for use of the ESRF. KT received a thesis grant from the Ministère de l'Education Nationale et de la Recherche.

References

Curien, G., Job, D., Douce, R. & Dumas, R. (1998). *Biochemistry*, **37**, 13212–13221.
Evans, G. & Pettifer, R. F. (2001). *J. Appl. Cryst.* **34**, 82–86.
Evans, P. R. (1997). *Proceedings of the CCP4 Study Weekend*, edited by K. S. Wilson, G. Davies, A. W. Ashton & S. Bailey, pp. 97–102. Warrington: Daresbury Laboratory.
Ferrer, J.-L., Simon, J.-P., Berar, J.-P., Caillot, B., Fanchon, E., Kaikati, O., Arnaud, S., Guidotti, M., Pirocchi, M. & Roth, M. (1998). *J. Synchrotron Rad.* **5**, 1346–1356.
Hendrickson, W. A., Smith, J. L. & Sheriff, S. (1985). *Methods Enzymol.* **115**, 41–55.
Jones, T. A., Zou, J. Y., Cowan, S. W. & Kjeldgaard, M. (1991). *Acta Cryst.* A**47**, 110–119.
La Fortelle, E. de, Irwin, J. J. & Bricogne, G. (1997). *Crystallographic Computing*, edited by P. Bourne & K. Watenpaugh, pp. 250–262. Oxford: IUCr.
Leslie, A. G. W. (1990). *Crystallographic Computing 5. From Chemistry to Biology*, edited by D. Moras, A. D. Podjarny & J.-C. Thierry, pp. 50–61. New York: Oxford Science Publications.
Lovell, S. C., Word, J. M., Richardson, J. S., & Richardson, D. C. (2000). *Proteins*, **40**, 389–408.
Otwinowski, Z. (1991). *Proceedings of the CCP4 Study Weekend. Isomorphous Replacement and Anomalous Scattering*, edited by W. Wolf, P. R. Evans & A. G. W. Leslie, pp. 80–86. Warrington: Daresbury Laboratory.
Otwinowski, Z. (1993). *Proceedings of the CCP4 Study Weekend. Data Collection and Processing*, edited by L. Sawyer, N. Isaacs & S. Bailey, pp. 56–62. Warrington: Daresbury Laboratory.
Sharff, A. J., Koronakis, E., Luisi, B. & Koronakis, V. (2000). *Acta Cryst.* D**56**, 785–788.
Sies, H., Klotz, L. O., Sharov, V. S., Assmann, A. & Briviba, K. (1998). *Z. Naturforsch. C*, **53**, 228–232.
Smith, J. L. & Thompson, A. W. (1998). *Structure*, **6**, 815–819.
Thomazeau, K., Curien, G., Dumas, R. & Biou, V. (2001). *Protein Sci.* **10**, 638–648.